Disruption of hippocampal–prefrontal cortex activity by dopamine D2R-dependent LTD of NMDAR transmission

Paul James Banks[a], Amelia Caroline Burroughs[a], Gareth Robert Isaac Barker[a], Jon Thomas Brown[b], Elizabeth Clea Warburton[a], and Zafar Iqbal Bashir[a,1]

[a]School of Physiology and Pharmacology, University of Bristol, Bristol, BS8 1TD, United Kingdom; and [b]Institute of Biomedical and Clinical Sciences, University of Exeter Medical School, Exeter, EX4 4PS, United Kingdom

Edited by Roberto Malinow, University of California, San Diego, La Jolla, CA, and approved July 27, 2015 (received for review June 25, 2015)

Functional connectivity between the hippocampus and prefrontal cortex (PFC) is essential for associative recognition memory and working memory. Disruption of hippocampal–PFC synchrony occurs in schizophrenia, which is characterized by hypofunction of NMDA receptor (NMDAR)-mediated transmission. We demonstrate that activity of dopamine D2-like receptors (D2Rs) leads selectively to long-term depression (LTD) of hippocampal–PFC NMDAR-mediated synaptic transmission. We show that dopamine-dependent LTD of NMDAR-mediated transmission profoundly disrupts normal synaptic transmission between hippocampus and PFC. These results show how dopaminergic activation induces long-term hypofunction of NMDARs, which can contribute to disordered functional connectivity, a characteristic that is a hallmark of psychiatric disorders such as schizophrenia.

medial prefrontal cortex | long-term depression | NMDA receptor hypofunction | D2R | schizophrenia

The hippocampus to medial prefrontal cortex (PFC) projection is important for executive function and working and long-term memory (1, 2). Glutamatergic neurons of the ventral hippocampal cornu ammonis 1 (CA1) region project directly to layers 2–6 of ipsilateral PFC, and this connection synchronizes PFC and hippocampal activity during particular behavioral conditions (3–5). Disruption of hippocampal–PFC synchrony is associated with cognitive deficits that occur in disorders such as schizophrenia (6). Hippocampal–PFC uncoupling can be achieved by NMDA receptor (NMDAR) antagonism (7), and NMDAR hypofunction is a recognized feature of schizophrenia (8). However, it is unclear, first, how changes in NMDAR function at this synapse may arise, and second, how NMDAR hypofunction affects hippocampal–PFC synaptic transmission.

Canonically, NMDARs are considered to contribute little to single synaptic events, but the slow kinetics of NMDARs contribute to maintaining depolarization, leading to the generation of bursts of action potentials (9–13). Furthermore, NMDARs coordinate spike timing relative to the phase of field potential oscillations (14, 15). NMDAR transmission itself undergoes synaptic plasticity (16, 17), and this can have a profound effect on sustained depolarization, burst firing, synaptic integration, and metaplasticity (9, 11, 18, 19). In PFC, NMDARs are oppositely regulated by dopamine receptors; D1-like receptors (D1Rs) potentiate and D2-like receptors (D2Rs) depress NMDAR currents (20). Interestingly, NMDAR hypofunction (8, 21) and dopamine D2 receptor activity (22) are potentially converging mechanisms contributing to schizophrenia (23).

We now examine the contribution of NMDARs to transmission at the hippocampal–PFC synapse. We show that NMDAR activity provides sustained depolarization that can trigger action potentials during bursts of hippocampal input to PFC. We next demonstrate that dopamine D2 receptor-dependent long-term depression (LTD) of NMDAR transmission profoundly attenuates summation of synaptic transmission and neuronal firing at the hippocampal–PFC input. These findings allow for a mechanistic understanding of how alterations in dopamine and NMDAR function can lead to the disruption of hippocampal–PFC functional connectivity, which characterizes certain psychiatric disorders.

Results

Role of NMDARs in Hippocampal–PFC Synaptic Transmission. In this study, we focus on the contribution of NMDARs to synaptic transmission at the hippocampal–PFC synaptic input. Experiments were conducted in slices of rat prefrontal cortex in which hippocampal–PFC fibers are preserved (see refs. 24, 25; Fig. S1 and Table S1). Layer 5 pyramidal neurons were current clamped at −70 mV, and single stimuli were applied to the hippocampal fiber tract [evoked excitatory postsynaptic potential (EPSP) mean amplitude, 3.2 ± 0.9 mV; $n = 10$]. The application of the NMDAR antagonist (D)-2-amino-5-phosphonopentanoic acid (AP5) did not affect peak EPSP amplitude (108 ± 16%; Fig. 1*A*; $P = 0.6$), but significantly reduced the 90–10% decay time of single EPSPs (from 67 ± 11 to 34 ± 4 ms, reduction to 56 ± 6% of control; Fig. 1*A*; $P = 0.003$), demonstrating NMDAR contribution to the duration of depolarization during a single EPSP. To examine the contribution of NMDAR activation to the summation of bursts of synaptic events, we delivered trains of 10 stimuli at different frequencies to the hippocampal afferents and measured the area under the summed EPSPs. AP5 significantly attenuated the synaptic response to 20 Hz (36 ± 6% of control;

Significance

Synaptic transmission between the hippocampus and prefrontal cortex is required for many executive cognitive functions. It is believed that disruption of this communication contributes to symptoms observed in psychiatric disorders including schizophrenia. Hyperdopaminergic tone and hypofunction of NMDA receptor-mediated glutamate transmission are distinctive elements of schizophrenia. Here we demonstrate that activation of low-affinity D2-like dopamine receptors leads to a lasting depression of NMDA receptors at the hippocampal–prefrontal projection of juvenile rats, leading to a marked disruption of synaptic transmission. These data demonstrate a link between dopamine and hypofunction of NMDA receptor-mediated transmission with potential implications for psychiatric disease.

Author contributions: P.J.B. and Z.I.B. designed research; P.J.B., A.C.B., G.R.I.B., and J.T.B. performed research; P.J.B. and E.C.W. analyzed data; and P.J.B. and Z.I.B. wrote the paper.

The authors declare no conflict of interest.

This article is a PNAS Direct Submission.

Freely available online through the PNAS open access option.

[1]To whom correspondence should be addressed. Email: Z.I.Bashir@bristol.ac.uk.

This article contains supporting information online at www.pnas.org/lookup/suppl/doi:10.1073/pnas.1512064112/-/DCSupplemental.

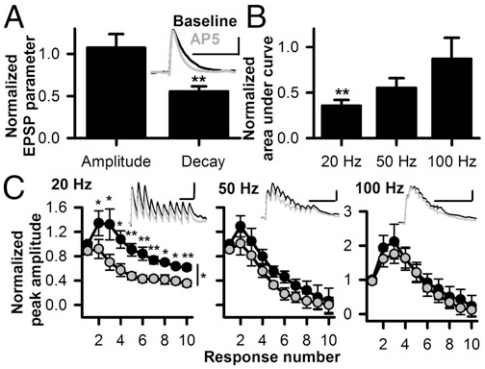

Fig. 1. NMDAR inhibition reduces temporal summation of hippocampal–PFC transmission. (*A*) AP5 (50 μM) reduces 90–10% decay time of single EPSPs [n = 10; paired t test $t_{(9)} = 3.96$; $P = 0.003$] without affecting peak amplitude [$t_{(9)} = 0.50$; $P = 0.63$]. (*Inset*) Before and after AP5 application. (*B*) Effect of AP5 on the area under the curve of EPSP bursts at different frequencies (n = 10). AP5 attenuates area under the curve at 20 Hz [paired t test $t_{(9)} = 3.39$; $P = 0.008$], but not at 50 Hz [$t_{(9)} = 1.63$; $P = 0.14$] or 100 Hz [$t_{(9)} = 1.36$; $P = 0.21$]. (*C*) Analysis of peak amplitude of each response during 20-, 50-, and 100-Hz bursts (nonspiking cells only, n = 7). Consistent with a lack of effect on single EPSP amplitude, response 1 was not affected by AP5 at 20 Hz [paired t test, $t_{(6)} = 1.98$; $P = 0.095$], 50 Hz [$t_{(6)} = 1.84$; $P = 0.12$], or 100 Hz [$t_{(6)} = 0.29$; $P = 0.78$]. Two-way repeated measures ANOVA (factors: drug, response number; Greenhouse-Geisser correction applied) of responses 2–10 showed a main effect of response number at 20 Hz [$F_{(1.13,6.81)} = 8.92$; $P = 0.019$], a main effect of drug [$F_{(1,6)} = 20.73$; $P = 0.004$], and crucially, a drug × response number interaction [$F_{(8,14.66)} = 3.72$; $P = 0.042$]. At 50 Hz, a main effect was shown for both factors [response number $F_{(1.06,6.37)} = 16.36$ ($P = 0.019$); drug $F_{(1,6)} = 11.05$ ($P = 0.016$)], but no interaction was observed [$F_{(1.632,9.791)} = 0.753$; $P = 0.471$]. At 100 Hz, a main effect was shown for response number [$F_{(1.36,8.14)} = 22.16$; $P = 0.001$], but not for drug [$F_{(1,6)} = 0.778$; $P = 0.412$], and there was no interaction [$F_{(1.66,9.94)} = 0.99$; $P = 0.389$]. (*Insets*) Example traces from same cell shown in *A*. (Scale bars, 100 ms/1 mV.) */** = $P < 0.05/0.01$, respectively.

Fig. 1 *B* and *C*; $P = 0.008$, paired t test), but not to 50 Hz (55 ± 11% of control; Fig. 1 *B* and *C*; $P = 0.14$) or 100 Hz (87 ± 23%; Fig. 1 *B* and *C*; $P = 0.2$; n = 10) stimulation.

As an alternative measure of summation of synaptic transmission, we determined the effect of AP5 on the amplitude of each EPSP during the bursts. This analysis was only performed on those cells that did not fire action potentials during the stimulation (n = 7/10). At 20 Hz stimulation, but not at 50 or 100 Hz, there was an overall decrease in temporal summation of EPSPs in the presence of AP5 compared with control conditions.

In some cells (3/10), burst stimulation of hippocampal afferents produced sufficient depolarization to elicit action potential firing. The presence of AP5 reduced the number of action potentials per stimulus train (Fig. S2*A*).

Thus, NMDAR-mediated transmission makes a significant frequency-dependent contribution to the synaptic activity of PFC neurons during hippocampal burst firing. In addition, NMDAR-mediated transmission makes a significant contribution to PFC neuronal spiking in response to hippocampal bursts.

LTD of NMDAR-Mediated Synaptic Transmission. Given the importance of NMDAR-mediated transmission to synaptic transmission during hippocampal burst activity demonstrated earlier, we examined how LTD of NMDAR-mediated transmission would affect hippocampal–PFC transmission. To first determine that plasticity of NMDAR transmission can occur at the hippocampal–PFC synapse, NMDAR-mediated EPSCs ($EPSC_{NMDA}$) were isolated by voltage-clamping cells at −40 mV and blocking AMPAR- and $GABA_A$R-mediated synaptic transmission with 5 μM 2,3-dioxo-6-nitro-1,2,3,4-tetrahydrobenzo[f]quinoxaline-7-sulfonamide (NBQX) and 50 μM picrotoxin, respectively.

Theta-frequency stimulation (TFS; 300 stimuli, 5 Hz, test intensity) resulted in lasting LTD of $EPSC_{NMDA}$ (to 58.5 ± 5.3% of baseline; Fig. 2*A*), which was not associated with a significant change in EPSC decay [baseline weighted tau = 164 ± 21 ms; post-TFS Tw = 204 ± 39 ms; paired t test $t_{(9)} = -0.95$; $P = 0.4$], indicating that LTD was unlikely to be associated with a switch in NMDAR subunits.

Importantly, TFS had no effect on $EPSC_{AMPA}$ (95.6 ± 6.4%; Fig. 2*B*). A two-way ANOVA (factors: receptor, stimulation) revealed a statistically significant interaction [$F_{(1,36)} = 15.9$; $P < 0.001$], indicating that TFS induces LTD specifically of NMDAR-mediated transmission. Furthermore, the paired pulse ratio of $EPSC_{NMDA}$ was not altered by TFS [baseline = 1.61 ± 0.1; post-TFS = 1.85 ± 0.18; n = 6; paired t test $t_{(5)} = -1.4$; $P = 0.22$]. This also suggests it is unlikely that LTD of $EPSC_{NMDA}$ is a result of a decrease in transmitter release.

We next examined which transmitters/receptors are responsible for LTD of $EPSC_{NMDA}$. Bath application of D2-like dopamine receptor antagonist sulpiride (10 μM) completely blocked the induction of LTD of $EPSC_{NMDA}$ (Fig. 2 *C* and *F*) but had no effect on basal transmission or maintenance of LTD (Fig. S3 *A* and *B*). In contrast, D1R-like antagonist SCH23390 (10 μM) did not block LTD (Fig. 2 *C* and *F*). Furthermore, the D1R-like agonist SKF81297 (0.5 μM) had no effect on $EPSC_{NMDA}$ (Fig. S4*A*), suggesting a differential role for D1 and D2Rs in regulation of NMDA receptors. Furthermore, bath application of the D2R agonist quinpirole (10 μM) also depressed $EPSC_{NMDA}$ (55.4 ± 2.8% of baseline; Fig. 2*D*). Delivery of TFS after quinpirole LTD had no significant effect on $EPSC_{NMDA}$ amplitude (60.6 ± 3.9%; Fig. 2*D*), suggesting quinpirole and TFS-LTD share common mechanisms. Together, these results suggest dopamine D2 receptors are critical for activity-dependent LTD of $EPSC_{NMDA}$.

To examine whether LTD of $EPSC_{NMDA}$ relied on NMDAR activation, neurons were voltage clamped at −100 mV during TFS, at which holding potential no $EPSC_{NMDA}$ was observed (Fig. S3*C*, *Inset*). Under these conditions, the induction of LTD still occurred (Fig. 2*E*, TFS at −100 mV; Fig. S3*C*). As a control, we show that hyperpolarization to −100 mV in the absence of TFS had no lasting effect on synaptic transmission (Fig. 2*E*, −100 mV control; Fig. S3*C*). Finally, delivering TFS in the presence of 50 μM AP5 did not prevent induction of LTD (Fig. 2*E*; AP5 + TBS; Fig. S3*D*). Together, these results suggest that LTD of $EPSC_{NMDA}$ does not require NMDAR activation.

We further investigated involvement of other G protein-coupled receptors in induction of NMDAR-LTD. Neither of the muscarinic receptor antagonists atropine (1 μM; Fig. 2*F* and Fig. S4*B*) and scopolamine (10 μM; Fig. 2*F* and Fig. S4*C*) prevented the induction of activity-dependent LTD. In addition, the broad-spectrum mGluR antagonist LY341495 (100 μM) did not prevent the induction of LTD (Fig. 2*F* and Fig. S4*D*).

D2-like dopamine receptors are coupled with inhibition of the adenylyl cyclase-cAMP-protein kinase A (PKA) pathway (20, 22, 26). Consistent with a key role of D2-like receptors in the generation of NMDAR-LTD, inhibition of PKA by bath application of H89 (10 μM) or KT5720 (200 nM) resulted in a slowly developing LTD of $EPSC_{NMDA}$ (Fig. 3*A*). Furthermore, prior activation of D2-like receptors with quinpirole markedly reduced subsequent depression by H89 (Fig. 3*B*), implying that D2 activation induces LTD via inhibition of PKA activity. Consistent with the lack of effect of the D1-like agonist SKF81297 upon $EPSC_{NMDA}$, the PKA agonist forskolin (10 μM) did not produce lasting effects on basal $EPSC_{NMDA}$ amplitude (Fig. 3*C*). Application of forskolin resulted in de-depression of $EPSC_{NMDA}$ when applied after prior TFS (Fig. S4*E*), implicating PKA inhibition in activity-dependent LTD of $EPSC_{NMDA}$. Previous studies have indicated that activation of glycogen synthase kinase3-beta (GSK3β) can result in depression of NMDAR transmission (27). However, we found that LTD of $EPSC_{NMDA}$ was unaffected by

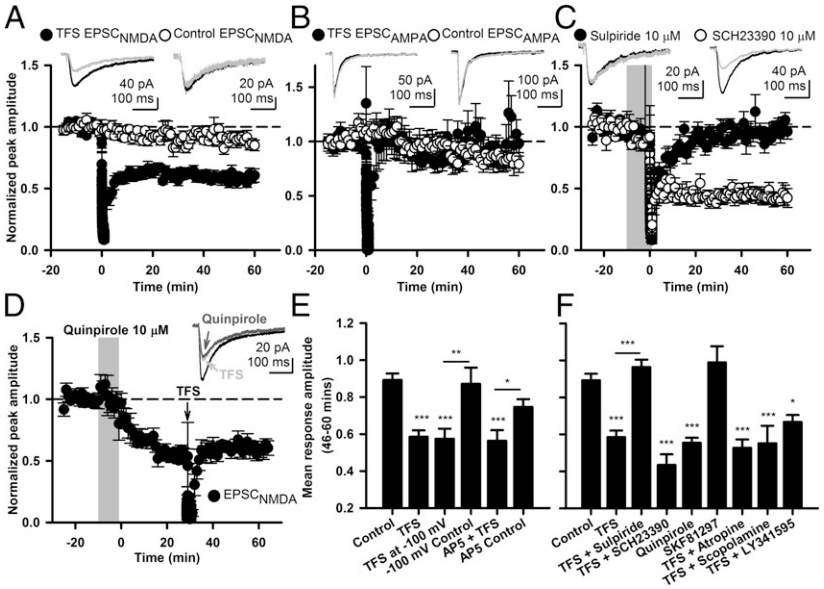

Fig. 2. TFS induces D2R-dependent LTD of EPSC$_{NMDA}$, but not of EPSC$_{AMPA}$. (*A*) Three hundred stimuli delivered at 5 Hz (TFS; delivered at time = 0 min, filled circles) induced LTD of hippocampal–PFC EPSC$_{NMDA}$ (depressed to 58.5 ± 5.3% of baseline; $n = 10$). Open circles: time-matched control NMDA EPSCs (89.3 ± 3.5%; $n = 13$). (*B*) TFS does not depress EPSC$_{AMPA}$ (filled circles; 95.6 ± 6.4%; $n = 10$) compared with time-matched control EPSC$_{AMPA}$ (open circles; 85.3 ± 8.2%; $n = 7$). (*C*) Induction of NMDAR-LTD was prevented by prior bath application (shaded region) of the D2-like dopamine receptor antagonist sulpiride (10 μM; filled circles; 96.3 ± 4.0%; $n = 5$; one-way ANOVA, Bonferroni post hoc vs. TFS alone; $P < 0.001$), whereas D1-like dopamine receptor antagonist SCH23390 (10 μM) failed to block induction of NMDAR-LTD (open circles, 43.4 ± 6.2%; $n = 5$; $P = 1.0$). (*D*) Bath application of D2-like dopamine receptor agonist quinpirole (10 μM) significantly depressed EPSC$_{NMDA}$ (55.4 ± 2.8%; $n = 5$; Bonferroni vs. control $P = 0.001$). Subsequent TFS failed to further depress EPSC$_{NMDA}$ [60.6 ± 3.9%; paired *t* test $t_{(4)} = -1.14$; $P = 0.316$]. (*E*) Summary of data in *A* and Fig. S3. LTD of EPSC$_{NMDA}$ by TFS does not require NMDAR activation. Hyperpolarization of cell to −100 mV during TFS does not prevent induction of NMDAR-LTD, and hyperpolarization to −100 mV alone does not alter EPSC$_{NMDA}$ amplitude. Blockade of NMDARs with AP5 (50 μM) before TFS does not prevent induction of NMDAR-LTD compared with AP5 applied without TFS. [One-way ANOVA, main effect $F_{(5,42)} = 14.62$; $P < 0.001$.] (*F*) Summary of data in *C* and *D* and Fig. S4. Bath application of D2R antagonist sulpiride prevents induction of NMDAR-LTD by TFS, whereas inhibition of D1Rs (SCH23390) does not. Pharmacological activation of D2Rs (quinpirole) induces LTD, but activation of D1Rs (SKF81297) has no effect. Muscarinic acetylcholine receptors (atropine, scopolamine) and mGluRs (LY341495) are not required for TFS-induced plasticity. One-way ANOVA main effect [$F_{(8,50)} = 14.76$; $P < 0.001$]. */**/*** = $P < 0.05/0.01/0.001$, respectively, Bonferroni post hoc compared against control group unless otherwise indicated. (*Insets*) Representative traces at baseline (black) and 46–60 min (gray).

either of the GSK3β inhibitors 2-methyl-4-(phenylmethyl)-1,2,4-thiadiazolidine-3,5-dione (TDZD-8) or SB216763 (Fig. S3*F*). In addition, inclusion of 1,2-bis(2-aminophenoxy)ethane-N,N,N′,N′-tetraacetic acid (BAPTA) in the patch pipette did not prevent the induction of LTD (10 mM; Fig. 3*D*). Thus, brief, 5-Hz stimulation results in LTD of EPSC$_{NMDA}$ that relies on dopamine D2 receptor activation and inhibition of cAMP/PKA.

Disruption of Hippocampal–PFC Transmission by LTD of NMDARs. We next examined the effects of TFS-induced LTD of NMDARs on single EPSPs and temporal summation of EPSPs at 20, 50, and 100 Hz at the hippocampal–PFC synapse 30–40 min after TFS. No change in peak amplitude of single EPSPs was detected after TFS (Fig. 4*A*). However, the decay time of single EPSPs was significantly decreased after TFS (Fig. 4*A*). The effects of TFS on peak amplitude and EPSP decay are consistent with the effects of AP5 on single EPSPs (Fig. 1*A*). Therefore, these data suggest that, as with the voltage-clamp experiments, TFS also induces robust LTD of NMDAR-mediated transmission under the current clamp conditions of the present experiments. In addition, these data also show that TFS is without effect on AMPAR-mediated transmission, which is consistent with the experiments showing that TFS delivered, under voltage-clamp conditions, results in LTD of EPSC$_{NMDA}$, but not EPSC$_{AMPA}$. (Fig. 2 *A* and *B*)

We then investigated the effects of NMDAR-LTD on summation of EPSPs (Fig. 4 *B* and *C*). Summation of synaptic transmission during 20-Hz stimulation was significantly reduced after TFS (area under the curve, 51.4 ± 4.6%; Fig. 4 *B* and *C*). Peak-by-peak analysis of EPSP trains evoked at 20 Hz also showed that amplitudes of responses 2–10 were reduced after TFS (Fig. 4*C*). Furthermore, TFS altered the short-term plasticity of the 20-Hz train (response × TFS interaction $P = 0.042$).

TFS significantly reduced synaptic summation at 50 Hz, as measured by the area under the curve (67 ± 19%; Fig. 4*B*); however, no significant effect was observed when analyzing peak amplitudes of burst responses (Fig. 4*C*). Summation of 100-Hz synaptic stimuli was not significantly affected by NMDAR-LTD (Fig. 4 *B* and *C*).

In four of 11 experiments, burst stimulation of hippocampal afferents produced sufficient depolarization to elicit spiking under control conditions (Fig. S2*B*). After TFS induced LTD of EPSC$_{NMDA}$, there was a reduction in the average number of action potentials per train of EPSPs (Fig. S2*B*).

Together, these results demonstrate that LTD of NMDAR transmission can disrupt, in a frequency-dependent manner, summation of hippocampal–PFC synaptic transmission and can attenuate subsequent action potential firing.

Disruption of Hippocampal–PFC Transmission by LTD of NMDARs Is Dependent on Activation of Dopamine D2Rs. Finally, we examined whether the disruption of synaptic transmission that occurred after TFS stimulation could be prevented by blocking LTD of EPSC$_{NMDA}$. Thus, the experiments described earlier were repeated in the presence of 10 μM sulpiride to block D2R-dependent induction of NMDAR-LTD. Under these conditions, TFS had no effect on EPSP decay (94 ± 7% of baseline; Fig. 5*A*). Summation of EPSPs in response to bursts of synaptic stimuli was not significantly reduced at any firing frequency, as measured

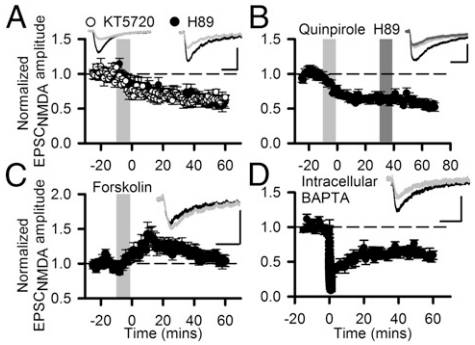

Fig. 3. NMDAR-LTD is mediated by PKA. (*A*) Inhibition of PKA mimicked the effect of D2-like dopamine receptor agonist quinpirole, producing a slowly developing LTD of $EPSC_{NMDA}$ in response to either H89 [10 μM; 58.7 ± 4.7%; $n = 5$; one-way ANOVA main effect $F_{(7,53)} = 13.76$; $P < 0.001$; Bonferroni vs. control, $P = 0.01$] or KT5720 (200 nM; 63.6 ± 5.3%; $n = 5$; Bonferroni vs. control, $P = 0.028$). (*B*) D2-like dopamine agonist quinpirole (10 μM, light gray shading and trace) depressed $EPSC_{NMDA}$ to 64.2 ± 3.8% ($n = 5$). Subsequent application of PKA inhibitor H89 (10 μM, dark gray shading and trace) resulted in a small further depression to 55.7 ± 2.5% of baseline [paired *t* test $t_{(4)} = 6.06$; $P = 0.004$]. The effect of H89 after quinpirole (8.6 ± 1.4% depression) was significantly smaller than that of H89 applied alone [38.8 ± 5.1% depression; *t* test $t_{(8)} = 5.67$; $P < 0.001$]. (*C*) PKA agonist forskolin induced a transient potentiation of $EPSC_{NMDA}$ (10 μM; amplitude 6–20 min postdrug = 128.4%; $P = 0.001$), which returned back to baseline levels within an hour of washout (107.3 ± 5.5%; $n = 8$; $P = 0.26$). (*D*) Inclusion of calcium chelator BAPTA in the intracellular recording solution did not prevent induction of NMDAR-LTD by TFS (10 mM; 61.7 ± 5.6%; $n = 5$; Bonferroni vs. TFS: $P = 1.0$). (*Insets*) Representative traces at baseline (black) and 46–60 min (gray). (Scale bars, 40 pA/100 ms.)

by area under curve (Fig. 5*B*) or by EPSP peak amplitudes (Fig. 5*C*). Finally, action potential firing was not altered after TFS in the presence of sulpiride (Fig. S2*C*).

These data show that activation of D2Rs results in LTD of NMDAR transmission that disrupts hippocampal–PFC synaptic activity. These results provide an insight into potential mechanisms by which dopamine receptor hyperfunction and NMDAR hypofunction might underlie the disruption of hippocampal–PFC synchrony that occurs in schizophrenia.

Discussion

The results of this study show that synaptic transmission from hippocampus to PFC is critically dependent on the activation of NMDARs in a frequency-dependent manner. Disruption of hippocampal–PFC transmission occurs after attenuation of NMDAR activity after application of AP5 or LTD of NMDAR-mediated synaptic transmission that relies critically on the activation of dopamine D2Rs. These results show that alterations in NMDAR function brought about by D2Rs contribute to disordered functional connectivity between hippocampus and PFC, a characteristic that is a hallmark of disorders such as schizophrenia.

NMDARs and Transmission Between Hippocampus and PFC. The hippocampal–PFC connection is critical in associative learning (2), and synchronization of PFC–hippocampal activity is important for working memory (5, 28, 29). We found that bursts of EPSPs at lower (20 Hz), but not higher (50 or 100 Hz), frequency are highly sensitive to NMDAR antagonism. Thus, NMDARs play a crucial role in determining the synaptic activity profile between hippocampus and PFC, maintaining the postsynaptic cell at depolarized membrane potential longer during 20 Hz transmission. Frequencies of ∼20 Hz occur in the hippocampus during spatial navigation (30), so NMDARs control synaptic transmission at physiologically relevant frequencies. In addition, NMDAR activation also contributed to spike firing in layer 5 PFC pyramidal neurons during bursting activity. Therefore, NMDAR activity controls hippocampal–PFC synaptic transmission and regulates the output of PFC pyramidal cells. Hence, NMDAR-dependent regulation of transmission between hippocampus and PFC may play an important role in associative and working memory.

LTD of $EPSC_{NMDA}$. Our data show that activity-dependent LTD of $EPSC_{NMDA}$ at the hippocampal–PFC synapse relies on endogenous activation of D2Rs. This significantly extends the physiological relevance of previous studies demonstrating that activation of D2Rs by exogenous agonists can depress NMDA agonist currents or NMDA EPSCs (27, 31–33). In contrast to the report that in 9–10-mo-old mice only a subpopulation of PFC pyramidal neurons express D2Rs (34), we found that in every case tested, LTD was D2R-dependent. Therefore, under the conditions of our experiments, it is unlikely that a large proportion of pyramidal neurons lack D2Rs. In contrast to previous reports of D1R-mediated enhancement of NMDAR transmission (20, 35), the application of a D1 agonist had no effect on the hippocampal–PFC $EPSC_{NMDA}$ in the present study. Although changes in NMDAR function in the hippocampus have been demonstrated to be dependent on muscarinic (36) and group I mGluR activation (37) the activity-dependent LTD in our study did not rely on activation of either of these receptor types.

Different mechanisms for D2R-dependent depression of NMDA responses have been suggested previously (32, 38). Although we were not able to confirm a role for GSK3β (27) in the D2R-dependent LTD of $EPSC_{NMDA}$, our results showing that the PKA inhibitor H89 depresses $EPSC_{NMDA}$ are consistent with a D2R-dependent inhibition of cAMP/PKA signaling being critical for

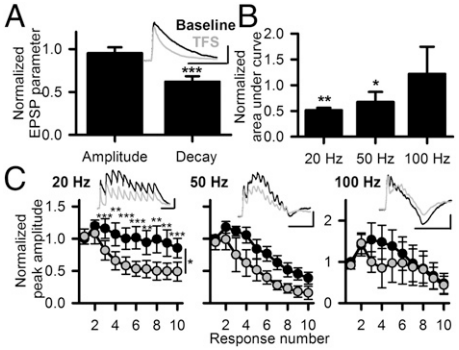

Fig. 4. TFS-induced NMDAR-LTD impairs temporal summation during burst stimulation. (*A*) TFS reduces the decay time of single EPSPs [57.1 ± 7.3% of baseline; $n = 11$; paired *t* test, $t_{(10)} = 5.49$; $P < 0.001$] without affecting peak amplitude [99 ± 7%; $t_{(10)} = 0.99$; $P = 0.345$]. (*B*) Thirty minutes after TFS, the area under the curve of 20 Hz [paired *t* test, $t_{(10)} = 4.64$; $P = 0.001$] and 50 Hz [$t_{(10)} = 3.10$; $P = 0.011$] synaptic bursts was reduced, whereas at 100 Hz, no effect was observed [$t_{(10)} = 0.313$; $P = 0.761$]. (*C*) Analysis of peak amplitude of each response during different frequency bursts (nonspiking cells only, $n = 8$ at 20 Hz; $n = 7$ at 50 and 100 Hz). Statistical analysis showed that the amplitude of response 1 was not affected by TFS at any frequency [repeated measures ANOVA 20 Hz: $F_{(2,16)} = 0.8$ ($P = 0.5$); 50 Hz: $F_{(2,12)} = 1.1$ ($P = 0.4$); 100 Hz: $F_{(1.170,7.020)} = 2.6$ ($P = 0.15$)]. Two-way repeated-measures ANOVA (factors: TFS, response number; Greenhouse-Geisser correction applied) of responses 2–10 in the 20-Hz burst showed a main effect of response number [$F_{(1.895,13.262)} = 15.7$; $P < 0.001$] and of TFS [$F_{(1,7)} = 73.0$; $P < 0.001$] and a response × TFS interaction [$F_{(2.030,14.210)} = 3.3$; $P = 0.042$]. At 50 Hz, a main effect of response number was found [$F_{(2.275,13.653)} = 12.1$; $P = 0.001$]; however, no significant main effect of TFS [$F_{(1,6)} = 5.3$; $P = 0.061$] or interaction [$F_{(2.221,13.325)} = 1.1$; $P = 0.4$] was observed. At 100 Hz, effects were not significant for response number [$F_{(1.762,10.57)} = 3.6$; $P = 0.07$], TFS [$F_{(1,6)} = 0.8$; $P = 0.4$] or their interaction [$F_{(2,11.997)} = 2.4$; $P = 0.13$]. */**/*** = $P < 0.05$, $P < 0.01$, $P < 0.001$, respectively. (*Insets*) Representative traces at baseline (black) and after TFS (gray). (Scale bars, 2 mV/100 ms.)

NEUROSCIENCE

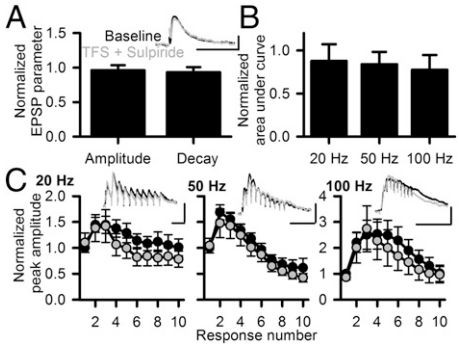

Fig. 5. D2R antagonism blocks TFS-induced effects on NMDAR transmission and TFS reduction in temporal summation. (*A*) In the presence of D2-like dopamine receptor antagonist sulpiride, TFS affects neither the peak amplitude [$n = 7$; paired t test, $t_{(6)} = 0.33$; $P = 0.75$] nor the decay time of individual EPSPs [$t_{(6)} = 0.419$; $P = 0.69$]. (*Inset*) Example EPSPs. (*B*) When delivered in the presence of sulpiride (10 μM), TFS had no effect on area under the curve of synaptic bursts at 20 [paired t test, $t_{(6)} = 1.36$; $P = 0.22$], 50 [$t_{(6)} = 1.42$; $P = 0.21$], or 100 [$t_{(6)} = 1.55$; $P = 0.17$] Hz. (*C*) Response by response analysis of temporal summation (nonspiking cells only) showed that peak amplitude changed as a function of response number at 20 Hz [two-way repeated-measures ANOVA, main effect of response number $F_{(2.381,16.667)} = 16.0$; $P < 0.001$], 50 Hz [$F_{(1.625,9.751)} = 14.1$; $P = 0.002$), and 100 Hz [$F_{(1.274,6.371)} = 8.3$; $P = 0.023$]; however, in the presence of sulpiride, no main effect of TFS was observed at any frequency [20 Hz: $n = 7$; $F_{(1,7)} = 4.7$; $P = 0.067$; 50 Hz: $n = 6$, $F_{(1,6)} = 1.8$, $P = 0.2$; 100 Hz: $n = 6$, $F_{(1,6)} = 1.8$, $P = 0.2$], nor were response × TFS interactions seen [20 Hz: $F_{(1.723,12.063)} = 1.7$ ($P = 0.2$); 50 Hz: $F_{(2.482,14.892)} = 0.3$ ($P = 0.8$); 100 Hz: $F_{(1.492,7.460)} = 2.9$ ($P = 0.12$)]. (*Insets*) Representative traces at baseline (black) and after TFS (gray). (Scale bars, 2 mV/100 ms.)

LTD (38). This finding for layer 5 PFC pyramidal cells is in contrast to a previous report suggesting a lack of cAMP/PKA signaling in D2R inhibition of NMDA currents in CA1 pyramidal neurons (31), but is in keeping with the mechanisms proposed to underlie the D2R-dependent decrease in NMDAR-dependent calcium influx in striatopallidal neurons (39).

That TFS resulted in LTD selectively of $EPSC_{NMDA}$, but not of $EPSC_{AMPA}$, indicates that LTD of NMDA transmission is not likely to rely on a decrease in transmitter release (39). Several mechanisms have been postulated for LTD of NMDARs, including internalization of receptors (37), diffusion of receptors to extrasynaptic sites (40), or a switch in NMDAR subunits (41). A recent report has suggested that prolonged D2R activation can decrease surface expression of NR2B-containing NMDARs in the CA1 region of hippocampus (42), and evidence suggests NR2B subunits have greater lateral mobility than NR2A (43). However, we found that LTD was not associated with a change in decay kinetics of $EPSC_{NMDA}$, suggesting no change in NMDAR subunit composition in our experiments. PKA activity has been shown to enhance NMDAR function via phosphorylation of NR1, NR2A, and NR2B subunits (44–46); thus, a reduction in PKA activity and subsequent dephosphorylation of NMDARs may provide a potential mechanism underlying the decrease in NMDAR currents (44).

Consequences of LTD of NMDAR for Synaptic Transmission. Activity-dependent plasticity of NMDAR transmission occurs at many synapses and can lead to metaplasticity (11, 18, 19). NMDAR plasticity may also play a homeostatic role. Plasticity of NMDAR transmission can accompany that of AMPA receptor (AMPAR) transmission, thereby preserving the AMPAR:NMDAR ratio (47). However, as TFS did not induce plasticity of AMPAR-mediated transmission, it is unlikely that the activity-dependent LTD of NMDARs fulfils a homeostatic function at the hippocampal–PFC input.

Aside from metaplasticity, a consequence of the long-term plasticity of NMDA transmission is the effect on synaptic transmission. We demonstrate that the normal EPSP summation and spike firing in layer 5 pyramidal neurons, driven by bursts of activity in hippocampal afferents, is significantly attenuated after activity-dependent LTD of NMDAR transmission. Previous studies have underlined the importance of NMDAR transmission in temporal summation between pairs of PFC pyramidal neurons, where they may play a key role in recurrent excitation (48) and persistent firing (49). Such effects may contribute to working memory processes in PFC. NMDA receptors also play a key role in integration of synaptic input in dendritic branches (10) and in the generation of plateau potentials, which can result in somatic spiking (50). Although temporal summation did not result in spiking in the majority of cases in this study, probably because of the relatively modest EPSP amplitude (~2–3 mV), NMDAR-mediated transmission may facilitate spatiotemporal integration of separate inputs in hippocampal neurons (51). Correspondingly, NMDAR LTD is likely to profoundly affect the input–output characteristics of PFC neurons receiving direct input from the hippocampus.

Implications of D2R-Induced LTD of NMDA. Dysfunction of the PFC is a widely reported phenomena in schizophrenia, in which the role of PFC in executive function and working memory is thought to be disrupted. Traditionally, hypotheses concerning mechanisms of schizophrenia have focused on dysfunction of the dopaminergic and glutamatergic systems, with D2R-like receptor hyperactivity (52) and NMDAR hypofunction (8, 53) being key features. Recently, it has been shown that cotreatment of patients with schizophrenia with both D2R-like antagonists and agents that increase NMDAR coagonist activity, such as D-serine or glycine transporter antagonists, are more effective than either treatment alone (54–56), supporting hypotheses of schizophrenia that include interaction of dopamine and NMDAR systems (21, 57, 58).

Here we present evidence that NMDAR transmission is a key driver of normal EPSP summation and action potential firing at the hippocampal–PFC projection where glutamatergic and dopaminergic projections converge on layer 5 pyramidal neurons (59, 60). D2R activation leads to a long-lasting reduction of NMDAR function in the hippocampal–PFC pathway that critically disrupts temporal summation at the hippocampal–PFC synapse and can lead to decreased PFC spiking in response to bursts of hippocampal activity. As there is evidence showing the importance of hippocampal–PFC signaling in working memory (5, 28, 29), associative memory (2), and executive function (61), cognitive faculties negatively affected in schizophrenia, we hypothesize that D2R-induced NMDAR hypofunction at the hippocampal–PFC pyramidal cells is a key dysfunction in the pathology of schizophrenia.

Materials and Methods

Animals. Experiments were conducted in male pigmented rats (Lister Hooded strain) postnatal day 30–32. All experiments were performed in accordance with the U.K. Animals (Scientific Procedures) Act 1986 and associated guidelines and had approval from the University of Bristol Ethics Committee. All efforts were made to minimize suffering and the number of animals used.

Electrophysiology. Rats were decapitated under isoflurane anesthesia, and the brain was removed and rapidly submerged in ice-cold (2–4 °C) oxygenated (95% O_2–5% CO_2) artificial cerebrospinal fluid (aCSF) containing (in mM): 124 NaCl, 3 KCl, 26 $NaHCO_3$, 1.25 NaH_2PO_4, 1 $MgSO_4$, 10 D-glucose, and 2 $CaCl_2$. The brain was cut at an 11° modified coronal angle using a custom brain matrix (Zivic Instruments), and 400-μm slices were made using a vibratome before storing in room temperature aCSF for ≥1 h before use. Slices equivalent to +2.7 to +2.2 mm from bregma were perfused with aCSF at 2 mL/min. Whole-cell patch clamp recordings were made from layer 5 neurons using 2–6-MΩ glass pipettes filled with either cesium

methylsulfonate-based solution (voltage clamp) or potassium gluconate-based solution (current clamp). Hippocampal–PFC responses were evoked by applying 0.1-ms constant current pulses to the hippocampal fiber tract, using a concentric bipolar stimulating electrode (24). Where applicable, NMDAR-mediated currents were isolated by bath application of picrotoxin (50 μM) and NBQX (5 μM) and voltage clamp of cells at −40 mV. Detailed information on electrophysiology and analysis can be found in *SI Materials and Methods*.

ACKNOWLEDGMENTS. This work was supported by the Wellcome Trust (Grant 087855/z/08/z) and the Biotechnology and Biological Sciences Research Council (BBSRC) (Grant BB/L001896/1).

1. Floresco SB, Seamans JK, Phillips AG (1997) Selective roles for hippocampal, prefrontal cortical, and ventral striatal circuits in radial-arm maze tasks with or without a delay. *J Neurosci* 17(5):1880–1890.
2. Barker GR, Warburton EC (2011) When is the hippocampus involved in recognition memory? *J Neurosci* 31(29):10721–10731.
3. Colgin LL (2011) Oscillations and hippocampal-prefrontal synchrony. *Curr Opin Neurobiol* 21(3):467–474.
4. Adhikari A, Topiwala MA, Gordon JA (2011) Single units in the medial prefrontal cortex with anxiety-related firing patterns are preferentially influenced by ventral hippocampal activity. *Neuron* 71(5):898–910.
5. O'Neill PK, Gordon JA, Sigurdsson T (2013) Theta oscillations in the medial prefrontal cortex are modulated by spatial working memory and synchronize with the hippocampus through its ventral subregion. *J Neurosci* 33(35):14211–14224.
6. Uhlhaas PJ, Singer W (2010) Abnormal neural oscillations and synchrony in schizophrenia. *Nat Rev Neurosci* 11(2):100–113.
7. Moran RJ, et al. (2015) Losing control under ketamine: Suppressed cortico-hippocampal drive following acute ketamine in rats. *Neuropsychopharmacology* 40(2): 268–277.
8. Javitt DC, Zukin SR (1991) Recent advances in the phencyclidine model of schizophrenia. *Am J Psychiatry* 148(10):1301–1308.
9. Augustinaite S, Heggelund P (2007) Changes in firing pattern of lateral geniculate neurons caused by membrane potential dependent modulation of retinal input through NMDA receptors. *J Physiol* 582(Pt 1):297–315.
10. Branco T, Häusser M (2010) The single dendritic branch as a fundamental functional unit in the nervous system. *Curr Opin Neurobiol* 20(4):494–502.
11. Hunt DL, Puente N, Grandes P, Castillo PE (2013) Bidirectional NMDA receptor plasticity controls CA3 output and heterosynaptic metaplasticity. *Nat Neurosci* 16(8): 1049–1059.
12. Lisman JE (1997) Bursts as a unit of neural information: Making unreliable synapses reliable. *Trends Neurosci* 20(1):38–43.
13. Polsky A, Mel B, Schiller J (2009) Encoding and decoding bursts by NMDA spikes in basal dendrites of layer 5 pyramidal neurons. *J Neurosci* 29(38):11891–11903.
14. Buzsáki G (2002) Theta oscillations in the hippocampus. *Neuron* 33(3):325–340.
15. Jensen O, Lisman JE (1996) Theta/gamma networks with slow NMDA channels learn sequences and encode episodic memory: Role of NMDA channels in recall. *Learn Mem* 3(2-3):264–278.
16. Bashir ZI, Alford S, Davies SN, Randall AD, Collingridge GL (1991) Long-term potentiation of NMDA receptor-mediated synaptic transmission in the hippocampus. *Nature* 349(6305):156–158.
17. Berretta N, et al. (1991) Long-term Potentiation of NMDA Receptor-mediated EPSP in Guinea-pig Hippocampal Slices. *Eur J Neurosci* 3(9):850–854.
18. Rebola N, Carta M, Lanore F, Blanchet C, Mulle C (2011) NMDA receptor-dependent metaplasticity at hippocampal mossy fiber synapses. *Nat Neurosci* 14(6):691–693.
19. Bhouri M, et al. (2014) mGlu1 receptor-induced LTD of NMDA receptor transmission selectively at Schaffer collateral-CA1 synapses mediates metaplasticity. *J Neurosci* 34(36):12223–12229.
20. Zheng P, Zhang XX, Bunney BS, Shi WX (1999) Opposite modulation of cortical N-methyl-D-aspartate receptor-mediated responses by low and high concentrations of dopamine. *Neuroscience* 91(2):527–535.
21. Lisman JE, et al. (2008) Circuit-based framework for understanding neurotransmitter and risk gene interactions in schizophrenia. *Trends Neurosci* 31(5):234–242.
22. Seamans JK, Yang CR (2004) The principal features and mechanisms of dopamine modulation in the prefrontal cortex. *Prog Neurobiol* 74(1):1–58.
23. Laruelle M, Frankle WG, Narendran R, Kegeles LS, Abi-Dargham A (2005) Mechanism of action of antipsychotic drugs: From dopamine D(2) receptor antagonism to glutamate NMDA facilitation. *Clin Ther* 27(Suppl A):S16–S24.
24. Parent MA, Wang L, Su J, Netoff T, Yuan LL (2010) Identification of the hippocampal input to medial prefrontal cortex in vitro. *Cereb Cortex* 20(2):393–403.
25. Wang L, Yuan LL (2009) Activation of M2 muscarinic receptors leads to sustained suppression of hippocampal transmission in the medial prefrontal cortex. *J Physiol* 587(Pt 21):5139–5147.
26. Goto Y, Yang CR, Otani S (2010) Functional and dysfunctional synaptic plasticity in prefrontal cortex: Roles in psychiatric disorders. *Biol Psychiatry* 67(3):199–207.
27. Li YC, Xi D, Roman J, Huang YQ, Gao WJ (2009) Activation of glycogen synthase kinase-3 beta is required for hyperdopamine and D2 receptor-mediated inhibition of synaptic NMDA receptor function in the rat prefrontal cortex. *J Neurosci* 29(49): 15551–15563.
28. Jones MW, Wilson MA (2005) Theta rhythms coordinate hippocampal-prefrontal interactions in a spatial memory task. *PLoS Biol* 3(12):e402.
29. Siapas AG, Lubenov EV, Wilson MA (2005) Prefrontal phase locking to hippocampal theta oscillations. *Neuron* 46(1):141–151.
30. Huxter J, Burgess N, O'Keefe J (2003) Independent rate and temporal coding in hippocampal pyramidal cells. *Nature* 425(6960):828–832.
31. Kotecha SA, et al. (2002) A D2 class dopamine receptor transactivates a receptor tyrosine kinase to inhibit NMDA receptor transmission. *Neuron* 35(6):1111–1122.
32. Liu XY, et al. (2006) Modulation of D2R-NR2B interactions in response to cocaine. *Neuron* 52(5):897–909.
33. Beazely MA, et al. (2006) D2-class dopamine receptor inhibition of NMDA currents in prefrontal cortical neurons is platelet-derived growth factor receptor-dependent. *J Neurochem* 98(5):1657–1663.
34. Gee S, et al. (2012) Synaptic activity unmasks dopamine D2 receptor modulation of a specific class of layer V pyramidal neurons in prefrontal cortex. *J Neurosci* 32(14):4959–4971.
35. Seamans JK, Durstewitz D, Christie BR, Stevens CF, Sejnowski TJ (2001) Dopamine D1/D5 receptor modulation of excitatory synaptic inputs to layer V prefrontal cortex neurons. *Proc Natl Acad Sci USA* 98(1):301–306.
36. Jo J, et al. (2010) Muscarinic receptors induce LTD of NMDAR EPSCs via a mechanism involving hippocalcin, AP2 and PSD-95. *Nat Neurosci* 13(10):1216–1224.
37. Snyder EM, et al. (2001) Internalization of ionotropic glutamate receptors in response to mGluR activation. *Nat Neurosci* 4(11):1079–1085.
38. Tritsch NX, Sabatini BL (2012) Dopaminergic modulation of synaptic transmission in cortex and striatum. *Neuron* 76(1):33–50.
39. Higley MJ, Sabatini BL (2010) Competitive regulation of synaptic Ca2+ influx by D2 dopamine and A2A adenosine receptors. *Nat Neurosci* 13(8):958–966.
40. Tovar KR, Westbrook GL (2002) Mobile NMDA receptors at hippocampal synapses. *Neuron* 34(2):255–264.
41. Matta JA, Ashby MC, Sanz-Clemente A, Roche KW, Isaac JT (2011) mGluR5 and NMDA receptors drive the experience- and activity-dependent NMDA receptor NR2B to NR2A subunit switch. *Neuron* 70(2):339–351.
42. Jia JM, Zhao J, Hu Z, Lindberg D, Li Z (2013) Age-dependent regulation of synaptic connections by dopamine D2 receptors. *Nat Neurosci* 16(11):1627–1636.
43. Groc L, et al. (2006) NMDA receptor surface mobility depends on NR2A-2B subunits. *Proc Natl Acad Sci USA* 103(49):18769–18774.
44. Aman TK, Maki BA, Ruffino TJ, Kasperek EM, Popescu GK (2014) Separate intramolecular targets for protein kinase A control N-methyl-D-aspartate receptor gating and Ca2+ permeability. *J Biol Chem* 289(27):18805–18817.
45. Maki BA, Cole R, Popescu GK (2013) Two serine residues on GluN2A C-terminal tails control NMDA receptor current decay times. *Channels (Austin)* 7(2):126–132.
46. Murphy JA, et al. (2014) Phosphorylation of Ser1166 on GluN2B by PKA is critical to synaptic NMDA receptor function and Ca2+ signaling in spines. *J Neurosci* 34(3):869–879.
47. Watt AJ, Sjöström PJ, Häusser M, Nelson SB, Turrigiano GG (2004) A proportional but slower NMDA potentiation follows AMPA potentiation in LTP. *Nat Neurosci* 7(5):518–524.
48. Wang H, Stradtman GG, 3rd, Wang XJ, Gao WJ (2008) A specialized NMDA receptor function in layer 5 recurrent microcircuitry of the adult rat prefrontal cortex. *Proc Natl Acad Sci USA* 105(43):16791–16796.
49. Ren M, Cao V, Ye Y, Manji HK, Wang KH (2014) Arc regulates experience-dependent persistent firing patterns in frontal cortex. *J Neurosci* 34(19):6583–6595.
50. Major G, Polsky A, Denk W, Schiller J, Tank DW (2008) Spatiotemporally graded NMDA spike/plateau potentials in basal dendrites of neocortical pyramidal neurons. *J Neurophysiol* 99(5):2584–2601.
51. Takahashi H, Magee JC (2009) Pathway interactions and synaptic plasticity in the dendritic tuft regions of CA1 pyramidal neurons. *Neuron* 62(1):102–111.
52. Seeman P, Lee T (1975) Antipsychotic drugs: Direct correlation between clinical potency and presynaptic action on dopamine neurons. *Science* 188(4194):1217–1219.
53. Olney JW, Newcomer JW, Farber NB (1999) NMDA receptor hypofunction model of schizophrenia. *J Psychiatr Res* 33(6):523–533.
54. Lane HY, et al. (2010) A randomized, double-blind, placebo-controlled comparison study of sarcosine (N-methylglycine) and D-serine add-on treatment for schizophrenia. *Int J Neuropsychopharmacol* 13(4):451–460.
55. Tsai G, Lane HY, Yang P, Chong MY, Lange N (2004) Glycine transporter I inhibitor, N-methylglycine (sarcosine), added to antipsychotics for the treatment of schizophrenia. *Biol Psychiatry* 55(5):452–456.
56. Tsai GE, Lin PY (2010) Strategies to enhance N-methyl-D-aspartate receptor-mediated neurotransmission in schizophrenia, a critical review and meta-analysis. *Curr Pharm Des* 16(5):522–537.
57. Lisman J (2012) Excitation, inhibition, local oscillations, or large-scale loops: What causes the symptoms of schizophrenia? *Curr Opin Neurobiol* 22(3):537–544.
58. Lewis DA, Moghaddam B (2006) Cognitive dysfunction in schizophrenia: Convergence of gamma-aminobutyric acid and glutamate alterations. *Arch Neurol* 63(10):1372–1376.
59. Sesack SR, Carr DB, Omelchenko N, Pinto A (2003) Anatomical substrates for glutamate-dopamine interactions: Evidence for specificity of connections and extrasynaptic actions. *Ann N Y Acad Sci* 1003:36–52.
60. Jay TM, Witter MP (1991) Distribution of hippocampal CA1 and subicular efferents in the prefrontal cortex of the rat studied by means of anterograde transport of Phaseolus vulgaris-leucoagglutinin. *J Comp Neurol* 313(4):574–586.
61. Gordon JA (2011) Oscillations and hippocampal-prefrontal synchrony. *Curr Opin Neurobiol* 21(3):486–491.
62. Paxinos G, Watson C (1998) *The Rat Brain In Stereotaxic Coordinates* (Academic, London), 4th Ed.
63. Anderson WW, Collingridge GL (2007) Capabilities of the WinLTP data acquisition program extending beyond basic LTP experimental functions. *J Neurosci Methods* 162(1-2):346–356.

Supporting Information

Banks et al. 10.1073/pnas.1512064112

SI Materials and Methods

General Surgical Procedure. All surgical procedures were performed on male Lister-hooded rats that weighed 300–400 g at the start of the procedure. Each rat was anesthetized with isoflurane [induction, 4% (vol/vol); maintenance, 2–3%] and secured in a stereotaxic frame with the incisor bar set at 3.3 mm below the interaural line. Injections of tracer or neurotoxin were made through burr holes at the coordinates outlined here. At the end of surgery, each animal received fluid replacement therapy (5 mL saline containing 1% glucose s.c.) and analgesia (0.05 mL Vetgesic i.m.).

Hippocampal Tracer Injection. Anterograde tracer (200 nL dextran-conjugated AlexaFluor488 4% in PBS; Life Technologies) was injected into the ventral hippocampus (−6.5 mm from bregma, −4.5 mm from midline, 6.4 mm below dura at an angle of 10° to the vertical plane) by pressure injection, using an UltraMicroPump 3 (World Precision Instruments) fitted with a 5-μL Hamilton syringe with a 33-gauge needle at a rate of 50 nL/min, with the needle left in situ for 10 min postinjection. Animals were anesthetized with sodium pentobarbital 7 d later and transcardially perfused with PBS followed by 4% paraformaldehyde and post-fixed in paraformaldehyde for 24 h and then transferred to 30% sucrose in 0.2 M phosphate buffer for 48 h before making coronal sections (40 μm) on a cryostat. Sections were mounted with Vectashield mounting medium (Vector Labs) containing 1.5 μg/mL DAPI. Images were obtained using a Leica DFC3000 FX camera mounted on a Leica DM5000B microscope with Leica GFP and A4 filter sets used to observe AlexaFluor488 and DAPI, respectively.

Hippocampal Lesions. Unilateral hippocampal excitotoxic lesions were made in six 300–400-g rats by making a series of injections of NMDA, as indicated in Table S1. Modified coronal slices were cut, as detailed here, 21–28 d after the lesions, and electrophysiological recordings were made from both hemispheres of PFC. The remaining tissue was fixed in paraformaldehyde for 48 h, transferred to 30% sucrose in 0.2 M PBS for 48 h, and sectioned at 40 μm on a cryostat before staining with cresyl violet. To determine the extent of the lesions, the remaining hippocampal tissue was measured in each hemisphere (Leica Qwin 3) in every fifth section between −1.9 and −6.3 mm relative to bregma, and the remaining hippocampal tissue from the lesioned hemisphere was expressed as a percentage of hippocampal tissue in the opposite hemisphere of the same sections.

Slice preparation. Animals were anesthetized with isoflurane and decapitated. The brain was rapidly removed and placed in ice-cold (2–4 °C) oxygenated (95% O_2–5% CO_2) aCSF containing (in mM): 124 NaCl, 3 KCl, 26 $NaHCO_3$, 1.25 NaH_2PO_4, 1 $MgSO_4$, 10 D-glucose, and 2 $CaCl_2$. The brain was cut at an 11° modified coronal angle, as described previously for the mouse (24), using a custom brain matrix (Zivic Instruments), and slices were cut at 400 μm using a vibratome before storing in room temperature aCSF for ≥1 h before use.

Electrophysiology. Slices equivalent to +2.7 to +2.2 mm from bregma (62) were transferred to a submerged recording chamber and perfused with aCSF at a rate of 2 mL/min. For voltage-clamp experiments, layer 5 neurons were patch clamped in the whole-cell configuration, using borosilicate glass (GC150F-10; Harvard Apparatus) electrodes 2–6 MΩ filled with a cesium methylsulfonate-based solution (in mM: 130 CsMeSO4, 8 NaCl, 10 Hepes, 0.5 EGTA, 4 Mg-ATP, 0.3 Na-GTP, 5 QX-314-Cl at pH 7.25, 280–295 mOsm) at room temperature. Recordings were obtained using an Axon Multiclamp 700B amplifier (Molecular Devices) and WinLTP v1.11b (63) or pClamp 10 (Molecular Devices) acquisition software, filtered at 4 kHz and digitized at 20 kHz (Digidata 1322A; Molecular Devices) without liquid junction potential correction. Cells in which series resistance exceeded 30 MΩ or changed >20% were discarded. A concentric bipolar stimulating electrode (CBAPB50; FHC) was placed on the hippocampal fiber bundle, and synaptic responses were evoked using 0.1-ms constant-current pulses. Picrotoxin (50 μM) and NBQX (5 μM) were bath applied and cells were held at −40 mV to isolate $EPSC_{NMDA}$. Activity-dependent LTD was induced by delivery of 300 pulses at 5 Hz at baseline stimulus intensity.

Current clamp recordings were performed at 31 ± 1 °C, using a potassium gluconate-based intracellular solution (in mM: 145 K-gluconate, 5 NaCl, 10 Hepes, 0.5 EGTA, 4 Mg-ATP, 0.3 Na-GTP at pH 7.25, 280–295 mOsm) and were acquired using pClamp10.2 software (Molecular Devices) low-pass filtered at 4 kHz and digitized at 100 kHz. Cells were held at −70 mV by injecting constant current (liquid junction potentials corrected post hoc), and single hippocampal–PFC EPSPs were evoked at 0.1 Hz before delivering synaptic trains of 10 stimuli delivered at 20, 50, and 100 Hz. In some experiments, NMDA receptors were blocked pharmacologically by bath applying 50 μM D-AP5 for 10 min before repeating synaptic measurements. In other experiments, TFS was applied by switching to voltage-clamp and stimulating 300 times at 5 Hz at $V_{holding}$ = −40 mV. Single responses and trains were then remeasured in current clamp during a 10-min period immediately after TFS, and again in a 10-min period 30 min after TFS.

Analysis. Data were analyzed using WinLTP and Clampfit (Molecular Devices) and statistical analysis using SPSS 21 (IBM). Results are expressed as mean ± SEM unless indicated otherwise. Statistical analysis of current clamp data were performed using repeated-measures ANOVA or paired *t* test. Statistical analysis of plasticity experiments was assessed by averaging data points from the last 15 min of the experiment, using one-way ANOVA with Bonferroni post hoc comparisons to allow inclusion of a control data group to account for effects of rundown. $EPSC_{NMDA}$ decay time constants were fit by a double exponential function using Clampfit and a weighted time constant (τ_w) calculated as $\tau_w = \tau_{fast}*[A_{fast}/(A_{fast} + A_{slow})] + \tau_{slow}*[A_{slow}/(A_{slow} + A_{fast})]$, where A = amplitude. τ_w were compared using paired *t* tests. Statistical significance was set at 0.05 for all comparisons. Statistical analysis of the effects of hippocampal lesions on electrophysiology were performed using Mann–Whitney nonparametric test.

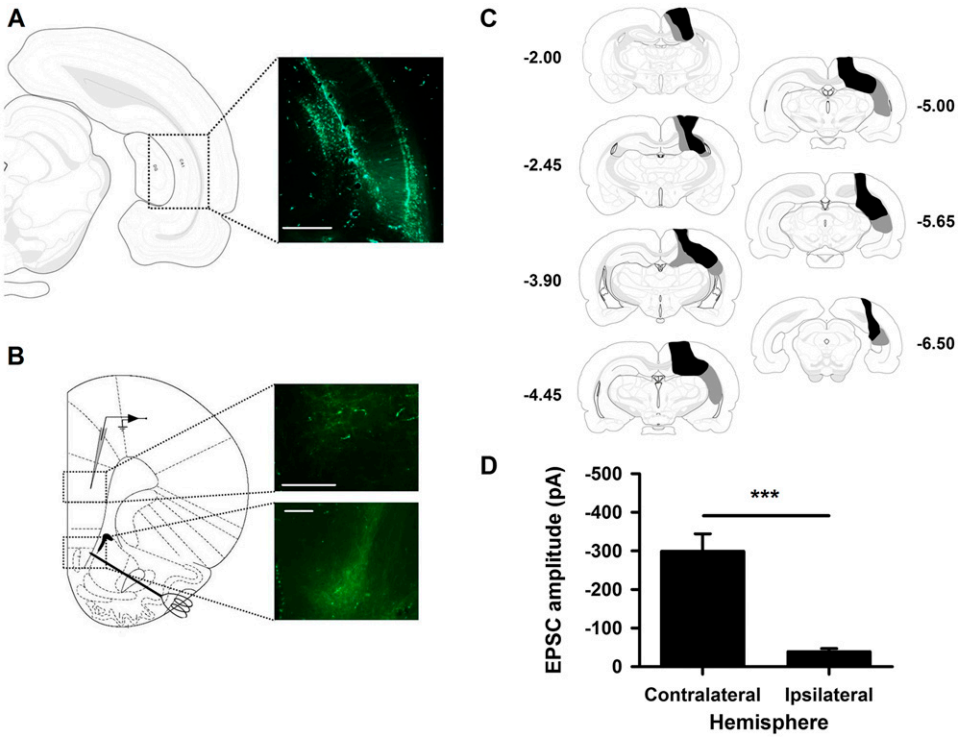

Fig. S1. Recording of hippocampal–PFC synaptic transmission in the rat in vitro. After labeling of the ventral hippocampal CA1 region with an anterograde tracer (*A*), fibers were observed running in a ventral–dorsal course (*B*, *Bottom Right*) and innervated infralimbic and prelimbic cortex (*B*, *Top Right*). Stimulation electrode is placed within hippocampal fiber bundle, and recordings made from prelimbic layer 5. (*C*) To confirm the origin of the putative hippocampal fiber bundle, unilateral excitotoxic lesions were made in six animals. Twenty-one days later, volumetric lesion analysis showed 61 ± 8% of hippocampal volume was lost. Largest (gray) and smallest (black) lesion volumes are shown. (*D*) In PFC slices contralateral to the lesion, stimulation of hippocampal afferents evoked large EPSCs in all cells (mean amplitude, 299 ± 45 pA; $n = 17$ cells from six animals), whereas in slices from the ipsilateral hemisphere, responses were absent or profoundly reduced in amplitude (38 ± 8.4 pA; $n = 19$ cells from six animals) compared with the contralateral hemisphere (Mann–Whitney test, $^{***}P < 0.001$).

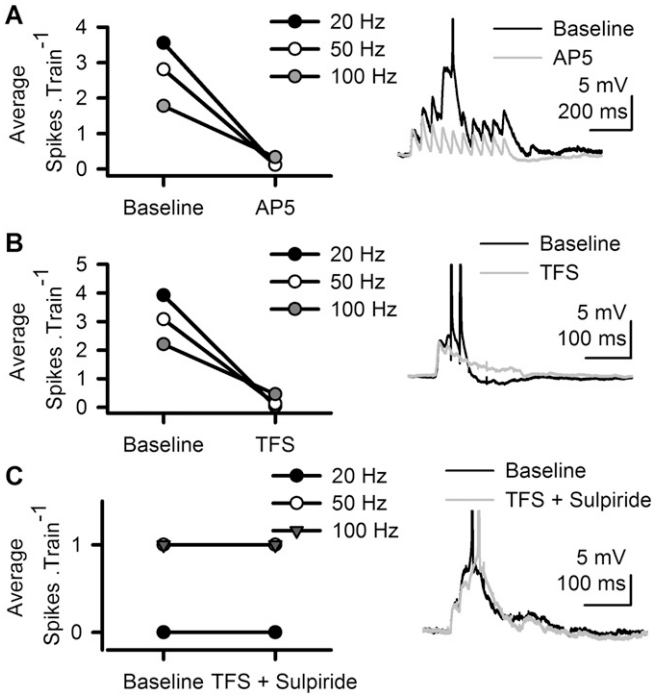

Fig. S2. Effects of NMDA receptor modulation on action potential firing. (*A*, *Left*) Plot of action potentials fired during synaptic bursts at different frequencies before and after bath application of AP5 (50 μM), averaged across three cells. (*Right*) Example trace of a cell that fires in response to a 20-Hz synaptic burst before, but not after, AP5. (*B*, *Left*) Action potentials fired before and after TFS averaged across four cells. (*Right*) Example traces of cell spiking in response to a 50-Hz synaptic burst with spiking attenuated after TFS. (*C*, *Left*) A single cell fired in response to 50- and 100-Hz synaptic bursts both before and after delivery of TFS in the presence of sulpiride. (*Right*) Example traces of 50-Hz bursts before and after TFS + sulpiride. Because of low experimental number, statistical analyses were not performed on these data.

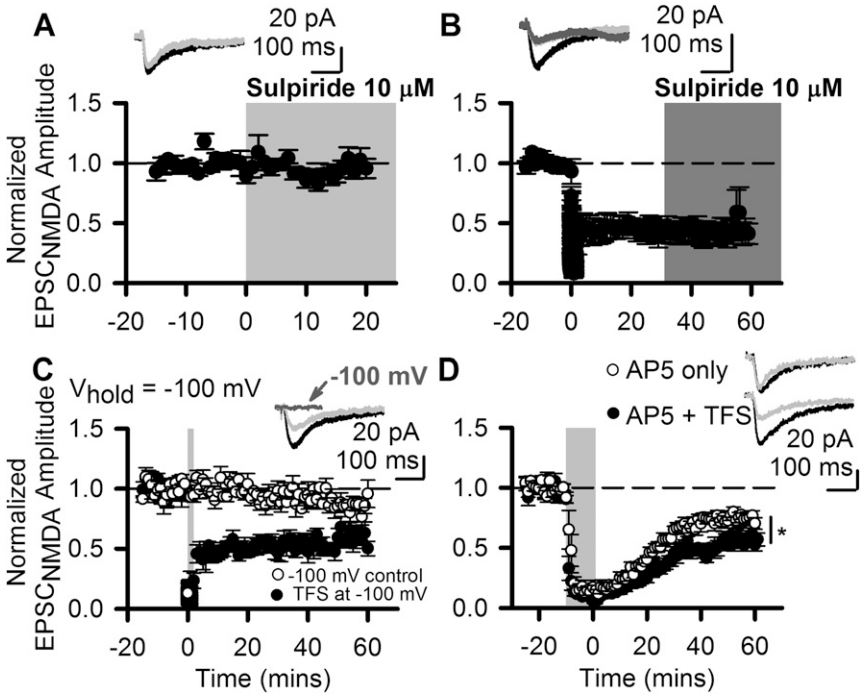

Fig. S3. D2-like dopamine receptor activation does not regulate basal NMDA transmission nor expression of NMDA-LTD, and induction of NMDA-LTD does not require activation of NMDARs. (*A*) Bath application of sulpiride (10 μM) had no effect on basal $EPSC_{NMDA}$ transmission [93.8 ± 4.5% of baseline; $n = 5$; paired t test $t_{(4)} = -1.127$; $P = 0.32$]. (*B*) The maintenance of LTD of $EPSC_{NMDA}$ (45.2 ± 8.2% of baseline; $n = 6$) is unaffected by sulpiride (10 μM), when bath applied 30 min later [44.7 ± 10.3% of baseline; paired t test $t_{(5)} = 0.192$; $P = 0.86$]. (*C*) Hyperpolarization of cell to −100 mV during TFS (shaded region) prevented ionic conductance through NMDARs (dark gray trace, *inset*), but did not prevent induction of NMDAR-LTD (filled circles, 57.4 ± 5.5% of baseline; $n = 5$; one-way ANOVA, Bonferroni post hoc vs. TFS, $P = 1.0$). Hyperpolarization to −100 mV in the absence of TFS was not sufficient to induce NMDAR-LTD (open circles, 87.1 ± 8.8%; $n = 4$; post hoc vs. TFS, $P = 0.002$; post hoc vs. control, $P = 1.0$). See Fig. 2*E* for summary. (*D*) Bath application of AP5 (50 μM, shaded region) before delivery of TFS did not prevent induction of LTD (filled circles, 56.4 ± 4.8%; $n = 8$; Bonferroni post vs. TBS alone, $P = 1.0$; control, $P < 0.001$). Furthermore TFS applied in the presence of AP5 was significantly different than a control group AP5 applied in the absence of TFS (open circles, 74.6 ± 2.7%; $n = 8$; Bonferroni post hoc, $P = 0.041$). The AP5 control group was not significantly different to time matched controls ($P = 0.11$). See Fig. 2*E* for summary. (*Insets*) Representative traces at baseline (black) and 46–60 min (gray).

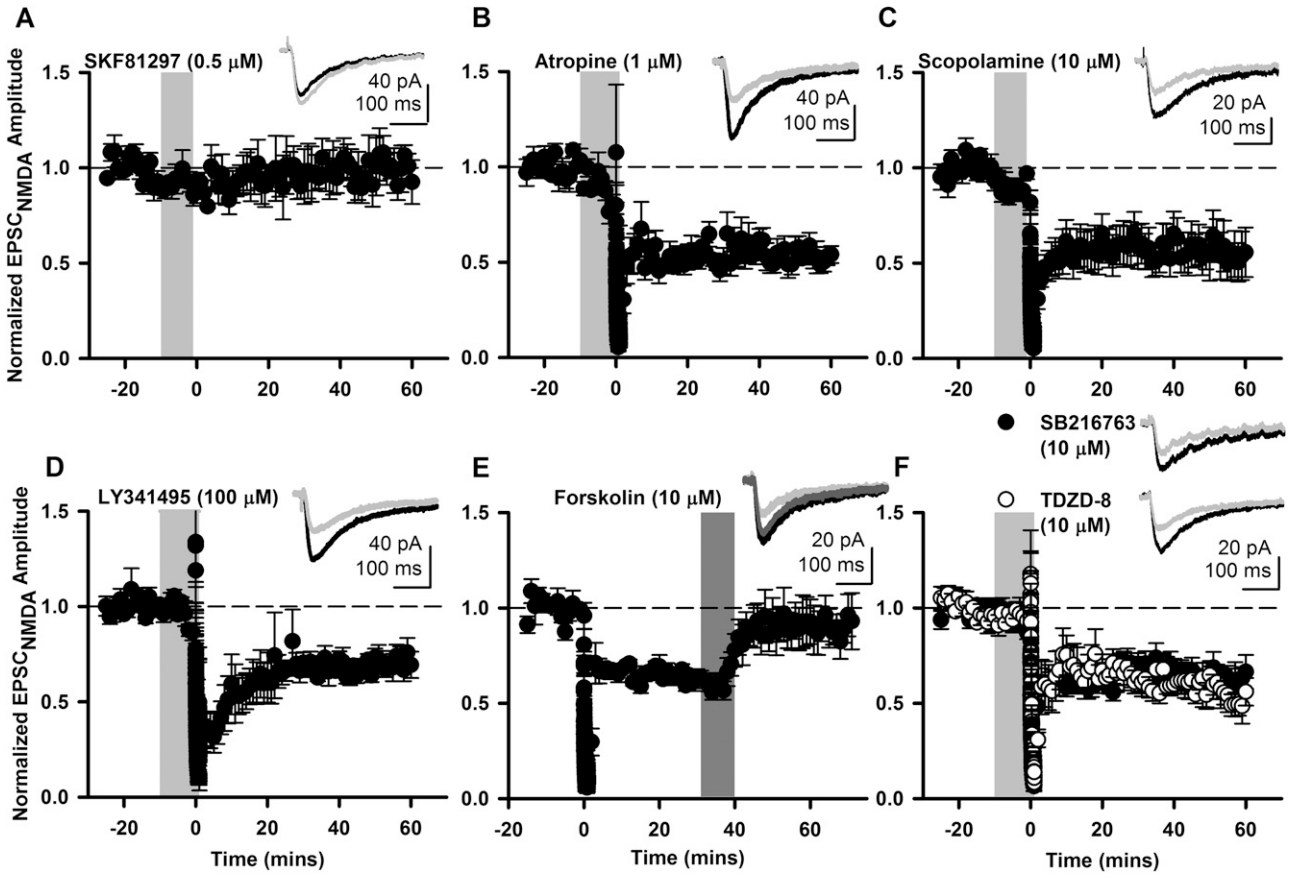

Fig. S4. (*A*) D1R-like dopamine receptor agonist SKF81297 (0.5 μM) had no effect on $EPSC_{NMDA}$ (98.9 ± 8.6% of baseline; $n = 5$; one way-ANOVA, Bonferroni vs. control, $P = 1.0$, vs. TFS, $P < 0.001$). Bath application of muscarnic acetylcholine receptor antagonists (*B*) atropine (1 μM, 52.7 ± 4.6%; $n = 5$; post hoc vs. TFS alone, $P = 1.0$) or (*C*) scopolamine (10 μM, 55.2 ± 9.4%; $n = 6$; post hoc vs. TFS alone, $P = 1.0$) did not prevent induction of LTD by TFS. (*D*) Bath application of LY341495 at a concentration (100 μM) that acts as a broad-spectrum mGluR antagonist did not prevent activity-dependent NMDAR-LTD (70.1 ± 4.6%; $n = 5$; post hoc vs. TFS alone, $P = 1.0$). (*E*) LTD of $EPSC_{NMDA}$ by TFS (64.8 ± 2.1%; $n = 5$; light gray trace) was reversed by bath application of forskolin [10 μM, dark gray trace, 90.8 ± 10.8% of baseline, paired *t* test, $t_{(4)} = -2.79$; $P = 0.495$]. (*F*) NMDAR-LTD induced by TFS was not blocked by bath application of GSK3β antagonists TDZD-8 (10 μM; 58.5 ± 7.1%; $n = 6$; Bonferroni vs. TFS, $P = 1.0$) or SB216763 (10 μM; 60.7 ± 5.6%; $n = 9$; post hoc vs. TFS alone, $P = 1.0$). (*Insets*) Representative traces at baseline (black) and 46–60 min (gray). (*A*–*D* are summarized in Fig. 2*F*).

Table S1. Injection coordinates for unilateral hippocampal lesions

AP	ML	DV	Volume, μL
−3.15	±1.0	−3.5	0.1
−3.45	±1.0	−3.7	0.1
−3.45	±2.5	−3.6	0.1
−4.75	±2.5	−3.0	0.1
−4.75	±4.0	−3.2	0.1
−4.75	±5.5	−4.0	0.1
−5.25	±2.5	−3.4	0.1
−5.25	±4.5	−4.0	0.15
−5.95	±4.6	−4.2	0.15
−6.35	±4.8	−5.0	0.15
−6.55	±4.8	−6.5	0.15
−6.75	±4.8	−6.5	0.15

Excitotoxic lesions were achieved by microinjection at 12 sites of 0.06 M NMDA dissolved in saline. Injections were made at a rate of 0.05 μL/min, and the needle was left in situ for either 2 (0.1 μL) or 3 min (0.15 μL). AP, anteroposterior; DV, dorsoventral; ML, mediolateral.